RSC Advances

ROYAL SOCIETY OF CHEMISTRY

www.rsc.org/advances

Cite this: DOI: 10.1039/c0xx00000x

www.rsc.org/xxxxxx

ARTICLE TYPE

Polymer controlled core-shell nanoparticles: A novel strategy for sequential drug release

Yang Cao, Bochu Wang,* Yazhou Wang and Deshuai Lou

Received (in XXX, XXX) Xth XXXXXXXXX 20XX, Accepted Xth XXXXXXXXX 20XX

DOI: 10.1039/b000000x

Sequential controlled drug release is required in cancer combination chemotherapy treatment. With the aim of co-delivering multiple drugs with different targets, immiscible and miscible liquids were utilized to fabricate PVP/PLGA and PCL/PLGA nanoparticles with distinct core-shell structure by coaxial electrospray. It allows the fabrication of core-shell nanoparticles with different inner core characteristics in hydrophilic properties in one single step. The anti-angiogenesis agent combretastatin A4 (CA4) and doxorubicin (DOX) were each encapsulated separately in the core and shell parts of dual-drug nanoparticles. Both hydrophobic and hydrophilic drugs can be encapsulated into the coaxi-electrosray particles effectively and the encapsulation efficiencies of drugs, particularly the hydrophilic ones, were over 90%. The endothelial cell and tumor cell co-culture systems were utilized to testify the performances of different nanoparticles in cytotoxicity, cellular apoptosis and VEGF and HIF-1α protein expressions *in vitro*. The melanoma cells B16-F10 and human umbilical vein endothelial cells (HUVECs) were sequentially targeted and killed by CA4 and DOX from these two kinds of nanoparticles. It demonstrated two different sequential drug release profiles *in vitro*. PVP/PLGA nanoparticles, with hydrophilic inner cores, presented a faster and higher drug release than that of PCL/PLGA nanoparticles, resulting from the better affinity of PVP polymers with incubation media. These results suggested that the release rates and profiles of dual drug loaded particles can be tailored and tuned by choosing core polymers with different characteristics in hydrophilic properties. Therefore, the clinical treatment necessity can be fulfilled and the improvement of drug efficiency is promising in tumor combination chemotherapy.

Introduction

In 2011, D. Hanahan and R. A. Weinberg have reported the hallmarks of cancer including sustaining proliferative signaling, evading growth suppressors, resisting cell death, enabling replicative immortality, inducing angiogenesis, and activating invasion andmetastasis.[1] These six biological capabilities are acquired during the multistep development of tumors, making it difficult to chemotherapy only by one singe agent. Meanwhile, it is known that cancer cells are able to acquire defense mechanisms by over expressing drug efflux pumps, enhancing self-repairing ability, increasing drug metabolism or expressing altered drug targets.[2-4] The efficacies of cancer chemotherapy are diminished. One of promising approaches is the combination chemotherapy by the co-delivery of various therapeutic agents in the same delivery vehicles.[5-23] In addition, therapeutic drugs should be used at optimal dosages for different periods to optimize the synergistic effects.[5, 10] Drug combinations releasing multiple drugs in a controlled manner are highly demanded.

It is promising for nanocarriers with core-shell structures to co-deliver multiply therapeutic agents. Multilayered or multi-compartmentalized microcapsules allow for simultaneous multiple drug delivery in biomedicine.[24-27] The microcapsules shell provided additional barriers to the diffusion of loaded drug in the core. The release rate was adjusted in this system by simply altering the amount of agents incorporated into scaffolds as well as polymer degradation time. Coaxial electrospraying with two separate feeding capillary channels is introduced, which can be utilized to deliver multiple drugs simultaneously. This technology would provide an alternative and simple means to produce core-shell systems without the need of surfactants or elevated temperatures.[28-32] Meanwhile, it has the potential to encapsulate therapeutic agents with different hydrophilic properties inside a core-shell polymeric particle, which supersedes other methods requiring two or more steps to achieve the encapsulated product.[33-34]

In polymer controlled drug delivery systems, the desired performance of vehicles is decided not only by the formulation of systems, but the most important by the structure and compatibility of carriers and drugs, which is remarkably influenced by the polymer hydrophilic properties and permeability characteristics of the polymer to the loaded molecules. With the aim of better know the sequential release profiles of core-shell nanoparticles, two kinds of core-shell nanoparticles were fabricated by coaxial electrospray in this paper. According to the affinity toward water, hydrophilic and hydrophobic polymers were chosen as carrier materials. Poly(lactic-co-glycolic acid) (PLGA), approved by FDA for

commercial application, is the most widely studied because of its sustained release characteristics, biocompatibility, and biodegradability. It was chosen as the shell polymer. The hydrophobic poly(ε-caprolactone) (PCL) and hydrophilic polyvinylpyrrolidone (PVP) were chosen as the core carriers. PCL and PVP have been reported to have lots of advantageous properties, such as good biodegradability and biocompatibility, good drug permeability and anti-fatigue capability, as well as low cost relative to other biodegradable polyesters.[35-36] The combination of antivascular therapy with anticancer chemotherapy has been reported to be a promising strategy to improve therapeutic index with reduced toxicity.[37] We chose combretastatin A4 (CA4) and doxorubicin (DOX) as model drugs for antivasculature and anticancer activities respectively. DOX is a cytotoxic drug commonly used in tumor treatments in clinic. It is supposed to be physically encapsulated into the core of nanoparticles. CA4, loaded into the PLGA shell, could cause a vascular shutdown.[36] In this study, coaxial electrospray was utilized to fabricate core-shell nanoparticles with immiscible and miscible liquids. DOX and CA4 were encapsulated in individual regions of nanoparticles respectively. The high encapsulation efficiencies of drugs were observed. The designed nanoparticles with different core polymers enabled two different temporal release profiles of two encapsulated drugs. This could enable to deliver multiple drugs according to clinical requirements.

Material and methods

Materials

Polyvinylpyrrolidone (PVP, K30, Mw: 50 000) was obtained from Sinopharm group Co. Ltd, China. PCL (Mw:80 000) and PLGA with lactide/glycolide molar ratio of 50:50 (PLGA, Mw: 50 000) were both purchased from Jinan Daigang Bio-Tech. Inc, China. DOX and CA4 were from Dalian Meilun Biology Technology Co., Ltd. (Dalian, China) and Hangzhou Great Forest Co., Ltd. (Hangzhou, China). Acetonitrile, tetrahydrofuran (THF) and N,N-dimethyl formamide (DMF) were procured from Chongqing Chuandong Chemical Reagents Co. Ltd, China. Phosphate-buffered saline (PBS) buffer used for *in vitro* release study and other reagents were all of analytical reagent grade, purchased from Chongqing Chuandong Chemical Reagents Co. Ltd, China.

The melanoma cells B16-F10 were generously provided from Prof. Bin Wang from the Third Military Medical University of P. R. China. Human umbilical vein endothelial cells (HUVECs) were obtained from College of Bioengineering, Chongqing University. The cells were maintained in RPMI 1640 medium supplemented with 10% fetal bovine serum (FBS) and 1% penicillin/streptomycin.

Nanoparticle fabrication by coaxial electrospray

Coaxial electrosraying was utilized to fabricate dual-drug loaded nanoparticles with core-shell structures, as shown in Fig.1. The inner/outer diameter of the core capillary was 0.3/0.5 mm. The inner diameter of outer capillary was 1.0 mm. The inner and outer fluid liquids were injected into two flow channels by two separate syringe pumps (TJ-3A, Longer, P. R. China). PLGA was chosen as outer material. PCL and PVP were used the inner polymers. A combination of THF and acetonitrile (2:8, v/v) was used as the organic solvent to dissolve PLGA. PCL was dissolved in acetonitrile. In order to increase the electrical conductivity of the solvent, DMF was added into the PVP ethanol solution (DMF: ethanol = 1:2, v/v). A voltage generator supplied a high voltage to the nozzle by means of a crocodile clip.

Electrospraying solutions and processing parameters were optimized to obtain nanoparticles of a stable cone-jet mode. In this study, the potential was 16 kV and the distance between the needle tip and the collector was 9 cm. The outer PLGA copolymer solution was 6% (w/v). The inner copolymer solution was 6% (w/v) PCL or 4% (w/v) PVP, respectively. 1% wt DOX and 4% wt CA4 were dissolved in the inner and outer electrospraying liquids, respectively. The dual-drug loaded nanoparticles were named as PCL-DOX/PLGA-CA4 and PVP-DOX/PLGA-CA4. The flow rates of inner and outer fluid liquids were 0.2 mL/h and 0.8 mL/h.

Fig.1.

Characterization of nanoparticles

The morphologies of nanoparticle surface were observed by field emission scanning electron microscopy (FE-SEM, Nova 400, FEI, America). For transmission electron microscope (TEM, FEI Tecnai 10, Philips Electron Optics, Holland), nanoparticle dispersions were deposited and dried on formvar film-coated copper grids after stained by phosphomolybdic acid hydrate. The dual-drug loaded nanoparticles were collected and suspended in anhydrous ethanol. Dynamic light scattering (DLS) methods were used to measure particle diameters and size distribution at 20 ^{o}C by Zetasizer Nano ZS 90 instrument (Malvern Instruments Ltd., Malvern, UK). The values of the same sample presented in the paper were average values of three-repeated measurement.

Drug encapsulation efficiency (EE) and in vitro release

The amount of drugs encapsulated in the composite particles was measured by dissolved the drug-loaded particles in 0.5 mL DMF. Add 2.5 mL PBS (pH 7.4) to the mixtures. The concentrations of the CA4 and DOX were determined using dual-wavelength spectrophotometer by UV spectrometry (Lambda 900, PerkinElmer, USA). DOX was determined at 483 nm and CA4 was measured using 298 nm as a characteristic wavelength and 453.8 nm as a reference one. The EE was defined as the ratio of actual and original amount of drug encapsulated in particles.

For drug release behaviors measurements, the drug-loaded particles was collected and incubated in a conical flask with 20 ml of pre-warmed PBS (100-120 rpm/min) at 37 ^{o}C. Due to the acidic of tumor microenvironment, two kinds of PBS at pH 7.4 and 6.5 were prepared. At designated time intervals, a 2-mL release medium was taken. The same amount of fresh buffer was then added in order to maintain the sink condition. The concentrations of CA4 and DOX were determined using dual-wavelength spectrophotometer as described previously. Accumulated release percentage of drug was determined as

$$Q(\%) = \frac{C_n \cdot V + V_i \sum_{i=0}^{n-i} C_i}{m_{drug}} \times 100\% \quad (1)$$

Here, Q (%) was the amount of accumulated release drugs. V (mL) was the total volume of samples. C_n (mg/mL) and V_i (mL) were the concentration and volume of samples taken at n and i time point. m_{drug} (mg) was the mass of drug in particles. The number of times of drug release media replacements was numbered as n.

In vitro tumor-endothelium co-culture studies

The cell co-culture flow chamber was developed based on parallel-plate-flow-chamber (Supplementary Material). HUVECs were cultured on the back side membrane of a transwell insert (6-well, 1μm) at density of 105 cells/insert and incubated at 37 °C, 5% CO2 for 4 h. B16-F10 cells were seeded in the top side membrane of the transwell chambers at a density of 10^5 cells/insert. The co-culture transwell chambers are able to allow the exchange of the medium. After 12h of incubation, the co-culture transwell chamber was installed on the parallel-plate-flow-chamber. The cell culture medium containing different nanoparticles was drawn out of the system by an infusion pump. The shear force of the medium was about 0.15-0.25 dynes/cm2. At the designed time point, B16-F10 cells and HUVECs were washed with cold PBS and collected.

Cytotoxicity assay and annexin V/propidium iodide cellular apoptosis

B16-F10 cells and endothelium cells were seeded in 96-well plates at 2×10^4 cells per well and incubated at 37 °C, 5% CO_2 for 24 h. The cells were exposed to the fresh culture medium containing respective samples (PCL-DOX/PLGA-CA4 and PVP-DOX/PLGA-CA4). The culture medium was replaced with 20μL MTT solution (5 mg/mL) and 180 μL serum free RPMI 1640 medium at the end of the incubation time (24 h, 48 h and 72 h). The plates were incubated for 4 h at 37 °C, 5% CO_2. Washing with PBS was followed by the addition of 150 μL DMSO to dissolve the formazan crystals, gentle shaking for 10-20 min so that complete dissolution was achieved. The absorbance was recorded at 490 nm using the microplate spectrophotometer system. The percent viability was expressed as absorbance in the presence of test compound as a percentage of that in the vehicle control.

Two-color flow cytometric analysis was used to study the cellular apoptosis after dual-drug nanoparticles treatments. B16-F10 cells and endothelium cells were collected at the end of incubation, respectively. Cells were washed with PBS and stained with reagents from Apoptosis Assay Kit (Bestbio Co. Ltd, China) following manufacturer's instruction and analyzed using a flow cytometer (FACS CantoTM II system; BD Biosciences, US).

Western blotting

B16-F10 cells and endothelium cells were seeded in 96-well plates at 2×10^4 cells per well and incubated at 37 °C, 5% CO_2 for 24 h. The cells were exposed to the fresh culture medium containing respective samples (PCL-DOX/PLGA-CA4 and PVP-DOX/PLGA-CA4). B16-F10 cells and endothelium cells were collected at the end of incubation, respectively. Cell samples were lysed in sample loading buffer and resolved on a 5-12% gradient SDS-polyacrylamide-gel electrophoresis gel. The proteins were transferred to a polyvinylidenefluoride (PVDF) membrane, blocked, and probed with the appropriate primary antibodies (SC-57496, SC-53546, Santa Cruz Biotechnology, Inc.) and secondary horseradish peroxidase-labelled antibodies (Products 31431, Thermo Scientific/Pierce Biotechnology, US). Proteins were detected by Enhanced Chemiluminescence Detection Kit for HRP (Beyotime Institute of Biotechnology, China). Quantitation of the chemiluminescent signals was performed with a digital imaging system (VersaDoc; Bio-Rad, US).

Statistic analysis

All the experiments were measured in triplicates and the results were presented as mean ± standard deviations. Statistical analyses of the experimental data from different groups were performed by applying one-way ANOVA. $p<0.05$ was considered significant, and $p<0.01$ was considered highly significant.

Results and discussion

Characterization of electrospraying particles

The surface morphologies and core-shell structure of particles were illustrated by SEM and TEM images (Fig.2 E-J). SEM images revealed that blank nanoparticles and dual-drug encapsulated nanoparticles were generally spherical and nearly monodisperse in size. The described core-shell structures were obtained for PVP/PLGA and PCL/PLGA nanoparticles from TEM. Clear boundaries between core and shell regions can be observed in these two kinds of nanoparticles. According to the results of DLS measurements (Fig.2 C-D), the average diameter of PVP/PLGA and PCL/PLGA nanoparticles was 394.7 nm (Pdi = 0.093) and 606.5 nm (Pdi = 0.289), respectively. It increased to 424.4 ± 78.9 nm and 455.7 ± 103.3 nm for PVP-DOX/PLGA-CA4 and PCL-DOX/PLGA-CA4 after CA4 and DOX encapsulated. It is believed that solvent evaporation and polymer diffusion are the two main mechanisms determining particle formation and their resulting properties.[38] Due to the different evaporation rate and diffusion rate between PCL solution and PVP solution, the different size distributions of these two systems were presented. As the dissolution of PLGA in ethanol was negligible, the polymer-solvent configuration was able to strongly reduce the diffusion between outer solution and inner solution at the tip of coaxial needle.[33] Meanwhile, the breakup process is greatly influenced by fluid properties such as electrical conductivity, viscosity, and interfacial tension.[39]

The zeta potential was strongly influenced by the properties of electrosray liquids as well. The surface charges of the dual-drug nanoparticles fabricated in this study were both negative (Supplementary Material Table S1). Due to the CA4 and Dox loading into the electrospray liquid, the zeta potentials of nanoparticles were varied. It has been reported that the zeta potential and surface charge of the nanoparticles directly affects

the physical stability, cellular uptake, biodistribution of the nanoparticles *in vivo*.[40] The negative zeta potential may help the dual-drug encapsulated nanoparticles to repel each other and prevent aggregation.[41] The crystallographic structure and chemical composition of PVP-DOX/PLGA-CA4 and PCL-DOX/PLGA-CA4 were revealed from the XRD analysis (Fig.3). There was no statistically significant difference in the diffractional peaks between blank nanoparticles and dual-drug loaded nanoparticles. Disappearance of the sharp peaks indicates distribution of the drug.

Fig.2

Fig.3

In vitro drug release profile studies

Owing to the advantages of coaxial-capillary electrosraying, it allows the encapsulation of multiple drugs in one single step, including drugs with different characteristics in hydrophilic properties. Hydrophobic CA4 and hydrophilic DOX were co-encapsulated in the core-shell nanoparticles (PCL/PLGA and PVP/PLGA) in this study. With different characteristics of core polymers in hydrophilic properties, PVP/PLGA and PCL/PLGA demonstrated variable release profiles (Fig. 4). As shown in Fig.4A, due to the hydrophilicity, 30% of DOX were released out within the first 2 hours of incubation in PBS at pH 7.4. Only 15% of CA4 were released out in 2 h. While, distinct property of release was observed in PCL-DOX/PLGA-CA4 as well. The release rate of DOX didn't change significantly when loading into PCL/PLGA nanoparticles. The release of CA4 from PCL-DOX/PLGA-CA4 was slower than CA4 release from PVP-DOX/PLGA-CA4. Due to the acidity of tumor microenvironments, drug release properties of dual-drug loaded nanoparticles were measured in the PBS at pH 6.5 as well. Compared with samples in pH 7.4 PBS, the release rates of DOX and CA4 from PCL-DOX/PLGA-CA4 nanoparticles were both decreased in pH 6.5 PBS. It showed that cumulative release percentages of encapsulated drugs were decreased from 55% to 48% for DOX, 30% to 20% for CA4 in the beginning 12 hours. In contrast, in PVP-DOX/PLGA-CA4, DOX release didn't change significantly in pH 6.5 PBS, whereas, the release of CA4 was reduced by 10%. The release in the following time was linear until 72 hours.

The initial drug release was attributed to the porosity of nanoparticles, resulting from the solvent evaporation in electrospray process. In addition, at higher loading, polymers were likely saturated with encapsulated drugs, leaving the remaining drug to precipitate between the carrier polymers and at the outer surface, which resulted in greater early release.[42] In the nanoparticles with core-shell structures, DOX was dispersed in the core regions, which had a longer path to release from the systems. However, this effect was diminished because the shell thickness was too small, which can be observed from TEM of nanoparticles. The release profiles of CA4 were shown due to the intermolecular force between PLGA and CA4 and low solubility in PBS solution. The CA4 solubility is poor in an aqueous medium so that it was hard to release from the nanoparticles. Thus, even if encapsulated in the core of nanoparticles, DOX had a higher cumulative release than that of CA4. Meanwhile, the strongly hydrophilic properties of PVP and large surface areas of nanoparticles were another two reasons for these observations.[43] The hydrophilic of PVP allows the water molecules to more easily penetrate into the center of nanoparticles. PVP might be dissolved from the nanoparticles into the aqueous medium. Some holes would be formed owing to the PVP dissolution so that much water could enter into the nanoparticles to promote the DOX release. In acidic microenvironment, the ionization molecules could induce and strengthen the polymer-drug interaction, resulting in decrease of drug release from nanocarriers.

Comparing with tradition drug loading methods, high encapsulation efficiency of encapsulated drugs was observed in coaxial-capillary electrosraying (Supplementary Material Table S2). In this study, both CA4 and DOX had high encapsulation efficiencies over 90% in PVP-DOX/PLGA-CA4 and PCL-DOX/PLGA-CA4. The results showed that the hydrophobic or hydrophilic properties of the drugs did not affect the amount of encapsulation with the coaxial-capillary electrosray method, as reported previously.[44-45] In another words, both hydrophobic and hydrophilic drugs can be encapsulated into the coaxi-electrosray particles effectively. The efficient encapsulation of drugs, particularly the hydrophilic ones, into the polymers with different hydrophilic properties is very promising.

Fig.4

Cytotoxicity assay

To investigate the cytotoxicity of blank nanoparticles, PCL/PLGA and PVP/PLGA nanoparticles were incubated with B16-F10 cells and HUVECs, respectively. As shown in Fig.5, there were no significant differences in cell morphology between the blank nanoparticles groups and controls. It showed that no significant decline in cell viability was detected on blank particle groups, suggesting the harmless of the blank nanoparticles. When the cell was treated with dual-drug loaded nanoparticles, it demonstrated various cell viabilities for different samples (Fig.6). Cell viability was significantly impaired when B16-F10 tumor cells were exposed to PVP-DOX/PLGA-CA4 at 0.5 mg/mL after 48 h treatment. As for HUVECs, the concentration of nanoparticles, leading to obvious cell cytotoxicity, increased to 1 mg/mL after the same time incubation. At the high nanoparticles concentration groups (2.5 mg/mL), it presented 48.76% cell viabilities of B16-F10 cells after 24 h incubation with PVP-DOX/PLGA-CA4. 49.44% HUVECs survived when treated with PVP-DOX/PLGA-CA4 after 24 h incubation. Since more drugs were released from the nanoparticles when treated at longer time, resulting in less cell viabilities. Cell viabilities of B16-F10 cells and HUVECs were decreased to 30.06%, 47.53% and 38.08%, 38.84% after 48 h and 72 h incubation with PVP-DOX/PLGA-CA4 at 2.5 mg/mL. In groups of PCL-DOX/PLGA-CA4 nanoparticles, it showed a dose-dependent and time-dependent manner as well. Compared with that of PVP/PLGA, lower cytotoxicity was detected in PCL-DOX/PLGA-CA4 treated groups, due to the low hydrophilicity and controlled release of encapsulated drugs from PCL/PLGA nanoparticles. When B16-F10 cells and HUVECs were treated with 2.5 mg/mL PCL-DOX/PLGA-CA4 nanoparticles after 48 h incubation, the cell viability was 62.16% and 54.54% remaining, respectively. Generally, it can be observed that both PCL-DOX/PLGA-CA4

and PVP-DOX/PLGA-CA4 demonstrated dose and time dependent toxicity on B16-F10 cells and HUVECs.

Fig.5

Fig.6

Apoptosis assay and western blot assay

Transwell cell co-culture systems were designed to study drug release profiles. As shown in Fig.7, apoptotic activities of B16-F10 cells and HUVECs were increased significantly from 24 h to 72 h for these two dual-drug loaded nanoparticles. It can be seen that the HUVECs cell apoptosis and became significant after 24 h incubation with PVP-DOX/PLGA-CA4 and PCL-DOX/PLGA-CA4, respectively. When B16-F10 cells were incubated with dual-drug loaded nanoparticles at different time, cell apoptotic activities increased sharply after 48 h incubation with PVP-DOX/PLGA-CA4 and 72 h for PCL-DOX/PLGA-CA4, respectively. This condition is consistent with the *in vitro* distinct drug release profiles of dual-drug delivery systems. Since the effective drug concentration was different for these two cell cultures. Although the cumulative of DOX was higher than CA4 release, the time inducing tumor cell apoptosis was later than HUVECs. Generally, the apoptosis assay showed that the sustained but continuous released DOX and CA4 maintained high cytotoxic activity for tumor cell and HUVECs apoptosis induction in a time-dependent manner. The sequential release of CA4 and DOX may allow more cytotoxic agents to accumulate in the tumor tissue before the tumor vasculatures collapse and have fewer side-effects, as previously studied.[46]

Fig.7 C-E showed the VEGF and HIF-1α protein expression of tumor cells at different incubation time. The expressions of VEGF and HIF-1α were both shut down when incubation with PVP-DOX/PLGA-CA4 nanoparticles after 24 hours. When tumor cells were treated with PCL-DOX/PLGA-CA4 nanoparticles, HIF-1α as well as VEGF protein expression was decreased after 48 h incubation significantly. It is known that low oxygen tension in tumors promotes neoangiogenesis by the activity of HIF-1α, a hypoxia-regulated transcription factor, over expression of which is associated with poor prognosis.[47] VEGF, a angiogenic factor, is potent chemoattractants for endothelium cells and for certain tumor cells that also express VEGF receptors.[48] As VEGF mediates endothelial cell survival functions, loss of VEGF signaling has been proposed to lead to endothelial cell apoptosis.[49]

In most tumors, the vasculature is characterized by a relatively inefficient blood supply which differs from normal vascular networks. Jain has hypothesized that tumor vasculature normalization may make the blood-flow more uniform with subsequent increased delivery of chemotherapy and oxygen.[50] In this study, two different sequential drug release profiles from PVP/PLGA and PCL/PLGA nanoparticles were observed. The different drug release rates and patterns were attributed to the distinct core-shell structures of nanoparticles and the difference of two core polymers in hydrophilic properties. PVP/PLGA nanoparticles presented a faster and higher drug release than that of PCL/PLGA nanoparticles, resulting from the better affinity of PVP with incubation media. It was easy for water molecules diffuse into the inner core of core-shell nanoparticles, which was the predominant rate step on drug release. CA4 was proposed to target tumor vasculature directly, which may result in redistributing blood flow and increasing overall delivery of chemotherapy and oxygen. The rest of the tumor cells were killed by the sustained-release of DOX from the nanoparticles. The sequential killing of the tumor endothelium and tumor cells can play a great powerful role in tumor combination chemotherapy.

Fig.7

Conclusions

The distinct core-shell structures were observed in PVP /PLGA and PCL /PLGA nanoparticles. DOX and CA4 were encapsulated in individual regions of nanoparticles with high encapsulation efficiency over 90%, respectively. The dual drug encapsulated nanoparticles had a narrow size distribution and smooth surface morphology. PVP-DOX/PLGA-CA4 and PCL-DOX/PLGA-CA4 exhibited different sequential release kinetics of encapsulated drugs. Treatment with dual-drug loaded nanoparticles resulted in the sequential killing of HUVECs and B16-F10 cells. The VEGF and HIF1-α expressions were both shut down *in vitro*.

Sequential controlled drug release is required in cancer combination chemotherapy treatment. In order to produce nanoparticles with multiple drugs encapsulated, the coaxial electrospray was employed. With the advantage of coaxial electrospray technology, immiscible and miscible liquids can be utilized to fabricate core-shell nanopartilces with different inner core characteristics in hydrophilic properties in one single step. Both hydrophobic and hydrophilic drugs can be encapsulated into the coaxi-electrosray particles effectively and the encapsulation efficiencies of drugs, particularly the hydrophilic ones, were increased. Owing to the carrier polymers with different characteristics in hydrophilic properties, drug release kinetics can be controlled. The cell co-culture system investigated has the potential to evaluate drug release or transport behaviors in mobile fluid. The results suggested that the release rates and profiles of dual drug loaded particles can be tailored and tuned by choosing required polymers with different characteristics. Therefore, the clinical treatment necessity can be fulfilled and the improvement of drug efficiency is promising in tumor combination chemotherapy.

Acknowledgment

This project was financially supported by the National Natural Science Foundation of China (Project Nos.: 31200713).

College of Bioengineering, Chongqing University, Chongqing 400030, PR China; Key Laboratory of Biorheological Science and Technology, Ministry of Education, Chongqing 400030, PR China.
** Corresponding author: Bochu Wang. Fax: +86-023-65112877; Tel:+86-023-65112840; E-mail: wangbc2000@126.com.*

References

1 D. Hanahan, R. A. Weinberg, *Cell*, 2011, **144**, 646-674.
2 M. M. Gottesman, *Annual Review of Medicine*, 2002, **53**, 615-627.
3 D. M. Bradshaw, R. J. Arceci, *Journal of Clinical Oncology*, 1998, **16**, 3674-3690.
4 S. Aryal, C. M. J. Hu, L. Zhang, *Molecular Pharmaceutics*, 2011, **8(4)**, 1401-1407.
5 L. Y. Qiu, Y. H. Bae, *Biomaterials*, 2007, **28**, 4132-4142.
6 L. Wei, C. Cai, J. Lin, T. Chen, *Biomaterials*, 2009, **30**, 2606-2613.

7 L. Zhang, A. F. Radovic-Moreno, F. Alexis, F. X. Gu, P. A. Basto, V. Bagalkot, S. Jon, R. S. Langer, O. C. Farokhzad, *ChemMedChem*, 2007, **2**, 1268-1271.

8 J. C. Wang, B. C. Goh, W. L. Lu, Q. Zhang, A. Chang, X. Y. Liu, T. M. Tan, H. Lee. *Biological & Pharmaceutical Bulletin*, 2005, **28**, 822-828.

9 A. Gursoy, E. Kut, S. Ozkirimli, *International Journal of Pharmaceutics,* 2004, **271**, 115-123.

10 Y. Wang, S. Gao, W. H. Ye, H. S. Yoon, Y. Y. Yang. *Nature Materials,* 2006, **5**, 791-796.

11 A. L. Z. Lee, Y. Wang, H. Y. Cheng, S. Pervaiz, Y. Y. Yang, *Biomaterials*, 2009, **30**, 919-927.

12 Z. Wang, P. C. Ho, *Biomaterials*, 2010, **31**, 7115-7123.

13 M. J. Vicent, F. Greco, R. I. Nicholson, A. Paul, P. C. Griffiths, R. Duncan, *Angewandte Chemie International Edition*, 2005, **44**, 4061-4066.

14 K. Miller, R. Erez, E. Segal, D. Shabat, R. Satchi-Fainaro, *Angewandte Chemie International Edition*, 2009, **48**, 2949-2954.

15 X. Song, Y. Zhao, W. Wu, Y. Bi, Z. Cai, Q. Chen, Y. Li, S. Hou, *International Journal of Pharmaceutics*, 2008, **350**, 320-329.

16 X. Song, Y. Zhao, S. Hou, F. Xu, R. Zhao, J. He, Z. Cai, Y. Li, Q. Chen, *European Journal of Pharmaceutics and Biopharmaceutics*, 2008, **69**, 445-453.

17 S. Aryal, C. M. J. Hu, L. Zhang, *Small*, 2010, **6**, 1442-1448.

18 A. J. Shuhendler, R. Y. Cheung, J. Manias, A. Connor, A. M. Rauth, X.Y. Wu, *Breast Cancer Research and Treatment*, 2009, **19**, 255-269.

19 J. Yang, C. H. Lee, H. J. Ko, J. S. Suh, H. G. Yoon, K. Lee, Y. M. Huh, S. Haam, *Angewandte Chemie International Edition*, 2007, **46**, 8836-8839.

20 Dilnawaz F, Singh A, Mohanty C, Sahoo SK., Biomaterials, 2010, **31**, 3694-3706.

21 L. Zhao, Y. Cheng, J. Hu, Q. Wu, T. Xu, *Journal of Physical Chemistry B*, 2009, **113**, 14172-14179.

22 Y. Ren, C. S. Kang, X. B. Yuan, X. Zhou, P. Xu, L. Han, G. X. Wang, Z. Jia, Y. Zhong, S. Yu, J. Sheng , P. Pu, *Journal of Biomaterials Science Polymer Edition*, 2010, **21**, 303-314.

23 S. Sengupta, D. Eavarone, I. Capila, G. Zhao, N. Watson, T. Kiziltepe, R. Sasisekharan, *Nature*, 2005, **436**, 568-572.

24 T. P. Richardson, M. C. Peters, A. B. Ennett, D. J. Mooney. *Nature Biotechnology*, 2001, **19**, 1029-1034.

25 M. Delcea, A. Yashchenok, K. Videnova, O. Kreft, H. Mohwald, A. G. Skirtach, *Macromolecular Bioscience*, 2010, **10**, 465-474.

26 H. Baumler, R. Georgieva, *Biomacromolecules*, 2010, **11**, 1480-1487.

27 M. Shi, Y. Y. Yang, C. S. Chaw, S. H. Goh, S. M. Moochhala, S. Ng, J. Heller, *Journal of Controlled Release*, 2003, **89**, 167-177.

28 V. T. Tran, J. P. Benoit, M. C. Venier-Julienne, *International Journal of Pharmaceutics*, 2011, **407**, 1-11.

29 N. K. Varde, D. W. Pack, *Expert Opinion on Biological Therapy*, 2004, **4**, 35-51.

30 I. D. Rosca, F. Watari, M. Uo, *Journal of Controlled Release*, 2004, **99**, 271-280.

31 A. Jaworek, A. T. Sobczyk, *Journal of Electrostatics*, 2008, **66**, 197-219.

32 Y. Z. Zhang, X. Wang, Y. Feng, J. Li, C. T. Lim, S. Ramakrishna, *Biomacromolecules*, 2006, **7**, 1049-1057.

33 H. Nie, Y. Fu, C. H.Wang , *Biomaterials*, 2010, **31**, 8732-8740.

34 H. Nie, Z. Dong, D. Y. Arifin, Y. Hu, C. H. Wang, *Journal of Biomedical Materials Research Part A*, 2010, **95A**, 709-716.

35 D. Li, J. X. Ding, Z. H. Tang, H. Sun, X. L. Zhuang, J. Z. Xu, X. S. Chen, *Internantional Journal of Nanomedicine*, 2012, **7**, 2687–2697.

36 D. Li, H. Sun, J. Ding, Z. Tang, Y. Zhang, W. Xu, X. Zhuang, *Acta Biomaterialia*, 2013, **9(11)**, 8875–8884.

37 T. M. Allen, P. R. Cullis*, Science*, 2004, **303**, 1818-1822.

38 J. Yao, L. K. Lim, J. Xie, J. Hua, C. H. Wang, *Journal of Aerosol Science,* 2008, **39(11)**, 987-1002.

39 Y. Lee, M. Bai, D. Chen, *Colloids and Surfaces B: Biointerfaces,* 2011, **82**, 104-110.

40 S. Acharya, F. Dilnawaz, S. K. Sahoo, *Biomaterials*, 2009, **30**, 5737-5750.

41 A. Singh, F. Dilnawaz, S. Mewar, U. Sharma, N. R. Jagannathan, S. K. Sahoo, *ACS Applied Materials & Interfaces*, 2011, **3**, 842-856.

42 Y. Zou, J. L. Brooks, V. Talwalkar, T. A. Milbrandt, D. A. Puleo, *Journal of Biomedical Materials Research Part B*, 2012, **100B**, 155-162.

43 S. W. AnnieáBligh, RSC Advances, 2013, **3**, 4652-4658.

44 H. Valo, L. Peltonen, S. Vehviläinen, M. Karjalainen, R. Kostiainen, T. Laaksonen, J. Hirvonen, *Small*, 2009, **5**, 1791-1798.

45 Y. Xu, M. A. Hanna, *International Journal of Pharmaceutics,* 2006, **320**, 30-36.

46 J. Zhang, L. Wu, H. K. Chan, W. Watanabe, *Advanced Drug Delivery Reviews*, 2011, **63**, 441-455.

47 G. L. Semenza, *Nature Reviews Cancer*, 2003, **3**, 721-732.

48 S. A. Eccles, *Current Opinion in Genetics & Development,* 2005, **15(1)**, 77-86.

49 L. M. Ellis, D. J. Hicklin, *Nature Reviews Cancer*, 2008, **8**, 579-591.

50 R. K. Jain, *Science*, 2005, **307**, 58-62.

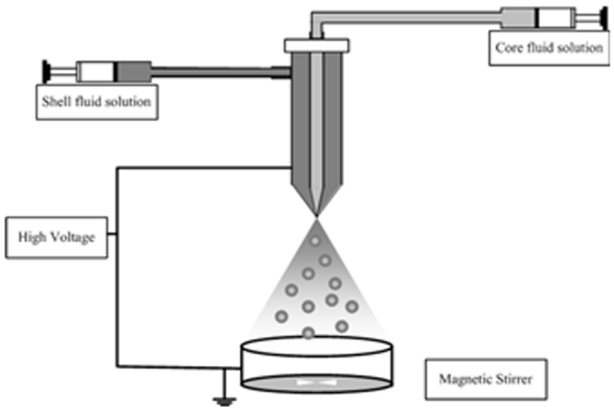

A schematic diagram of the coaxial electrospray system

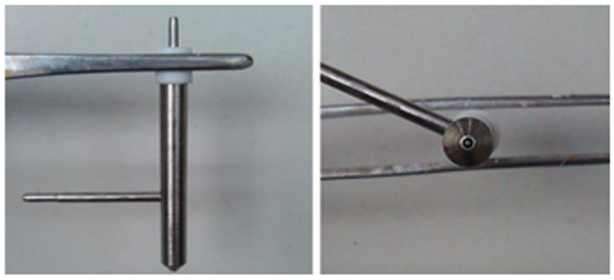

Figure of the coaxial capillary

Fig.1. A schematic diagram of the coaxial electrospray system for core-shell nanoparticle fabrication

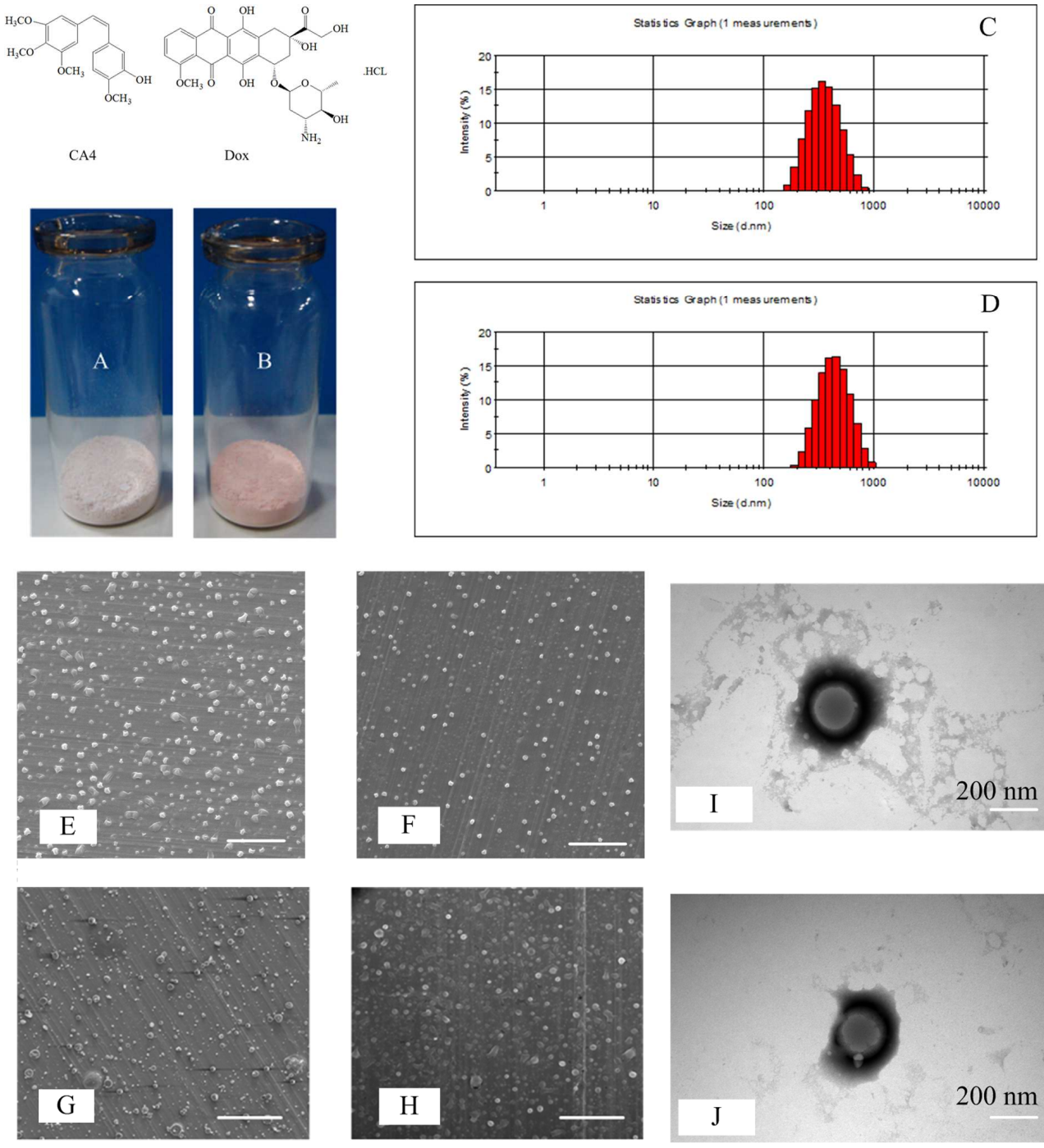

Fig.2 Nanoparticles characterization. A-B) Figures of drug loaded nanoparticles A: PCL-DOX/PLGA-CA4; B: PVP-DOX/PLGA-CA4; C-D) Size distribution of dual drug loaded nanoparticles C: PVP-DOX/PLGA-CA4; D: PCL-DOX/PLGA-CA4; E-H) SEM of nanoparticles E: PCL/PLGA nanoparticles; F) PVP/PLGA nanoparticles; G) PCL-DOX/PLGA-CA4; H) PVP-DOX/PLGA-CA4; Scar bar =5 μm; I-J) TEM of nanoparticles I: PCL-PLGA; J: PVP-PLGA; Scar bar = 200 nm.

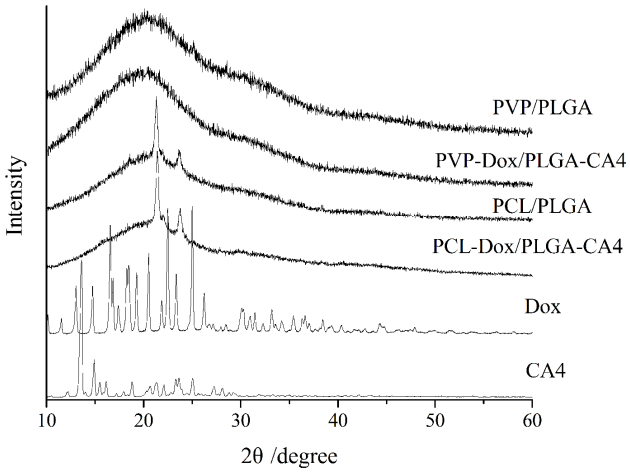

Fig.3 XRD curves of nanoparticles

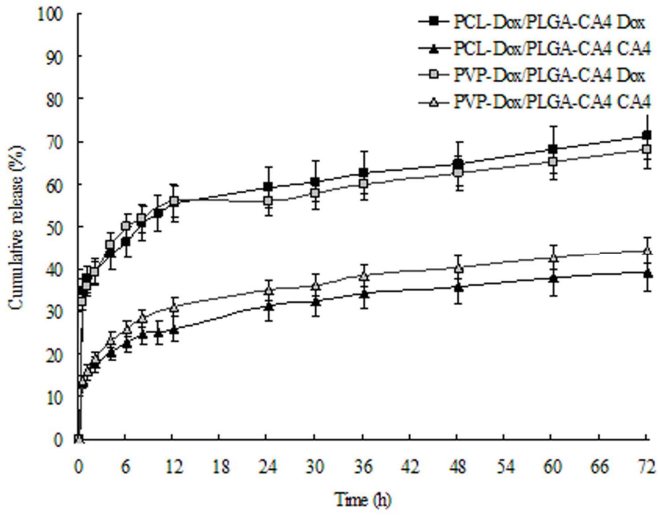

Fig.4A Release profiles of dual drug-loaded polymer particles in PBS（pH=7.4）

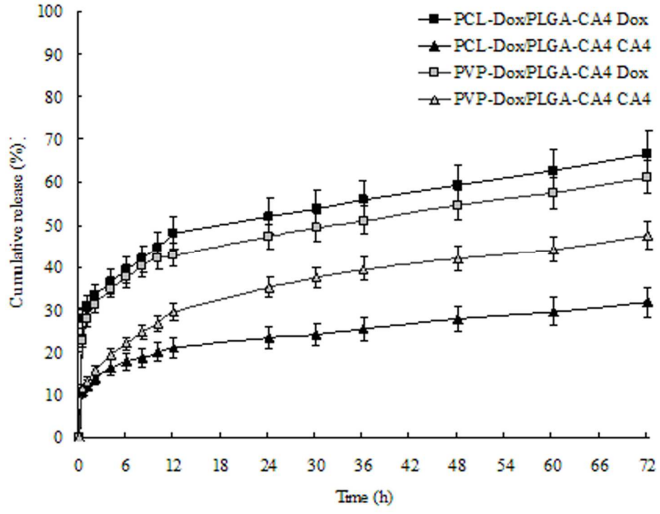

Fig.4B Release profiles of dual drug-loaded polymer particles in PBS（pH=6.5）

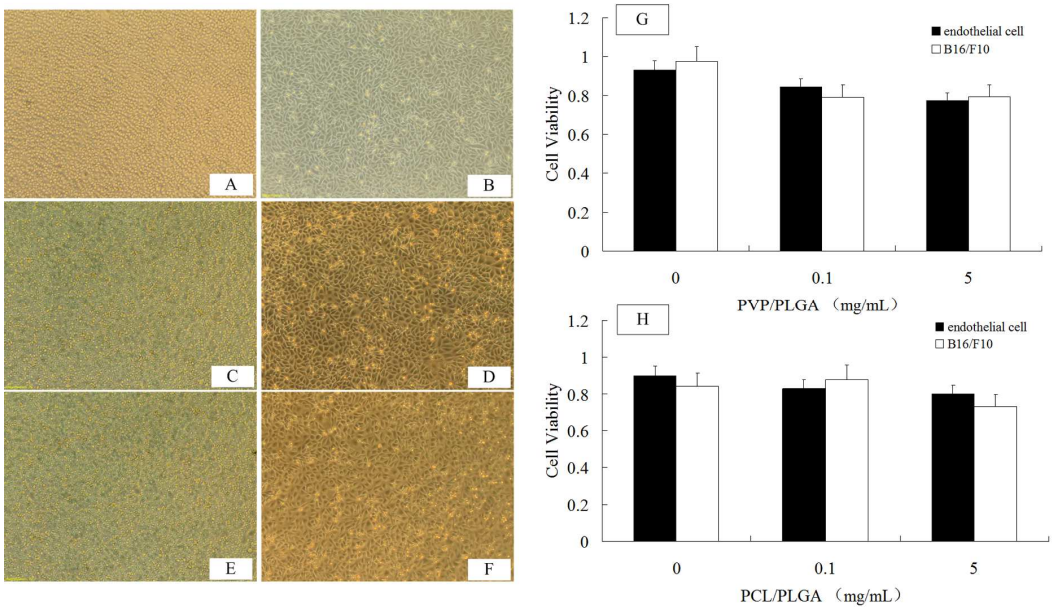

Fig.5 A-F) Morphology of B16-F10 and EC after 48h incubation with nanoparticles *in vitro* A: B16-F10; B: EA.HY926; C: B16-F10 + PCL/PLGA; D: EA.HY926 + PCL/PLGA; E: B16-F10 + PVP/PLGA; F: EA.HY926 + PVP/PLGA; G-H) Cytotoxicity of nanoparticles after 48h incubation *in vitro* G: PVP/PLGA; H: PCL/PLGA.

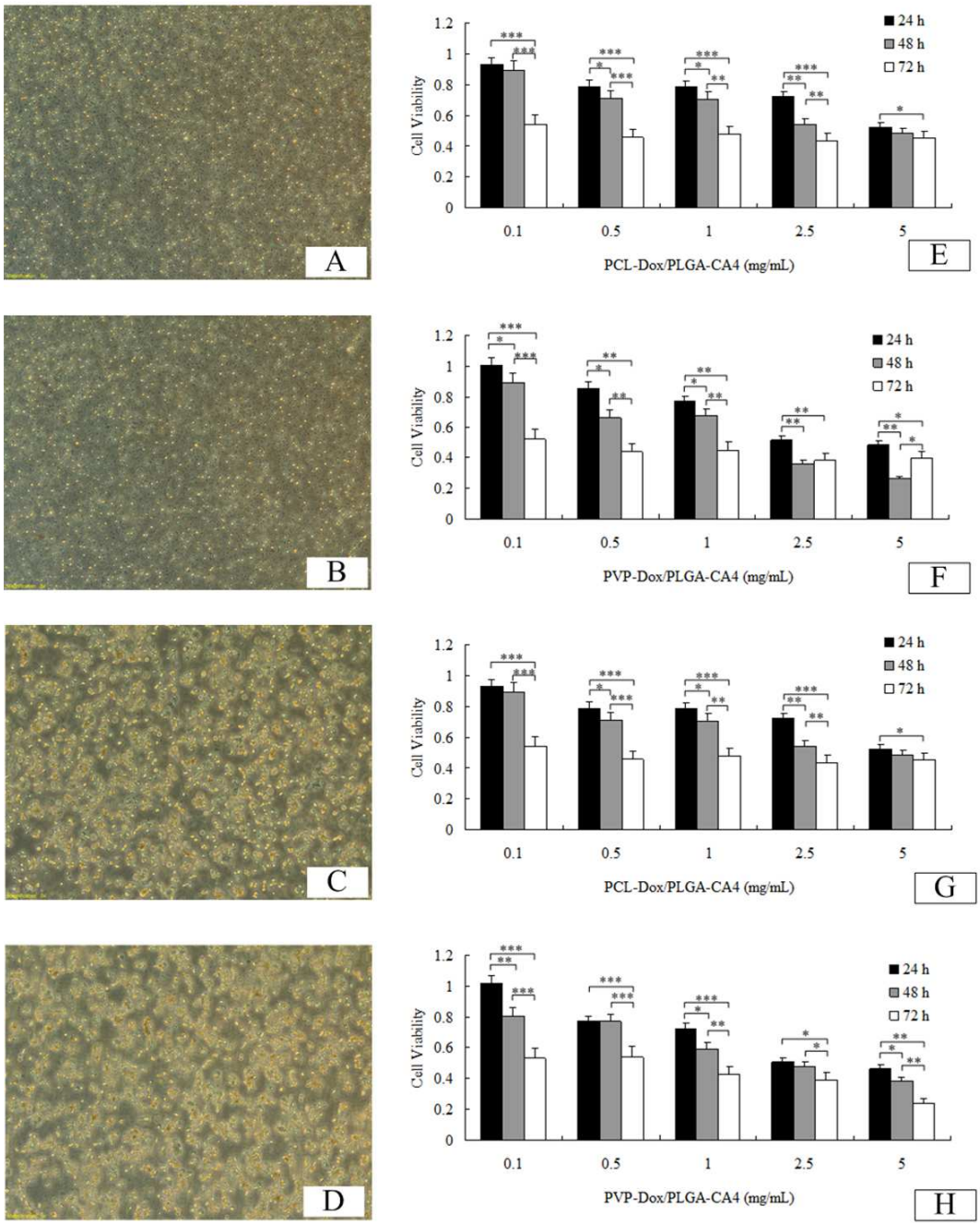

Fig.6 A-D) Morphology of B16-F10 and EA.HY926 after 48h incubation with nanoparticles *in vitro* A: B16-F10 + PCL-DOX/PLGA-CA4; B: B16-F10 + PVP-DOX/PLGA-CA4; C: EA.HY926 + PCL-DOX/PLGA-CA4; D: EA.HY926 + PVP-DOX/PLGA-CA4; E-H) Cytotoxicity of B16-F10 and EA.HY926 after incubation with nanoparticles *in vitro* E: B16-F10 + PCL-DOX/PLGA-CA4; F: B16-F10 + PVP-DOX/PLGA-CA4; G: EA.HY926 + PCL-DOX/PLGA-CA4; H: EA.HY926 + PVP-DOX/PLGA-CA4; (mean ± SD; n = 4) * P <0.05, ** P<0.01, *** P<0.001.

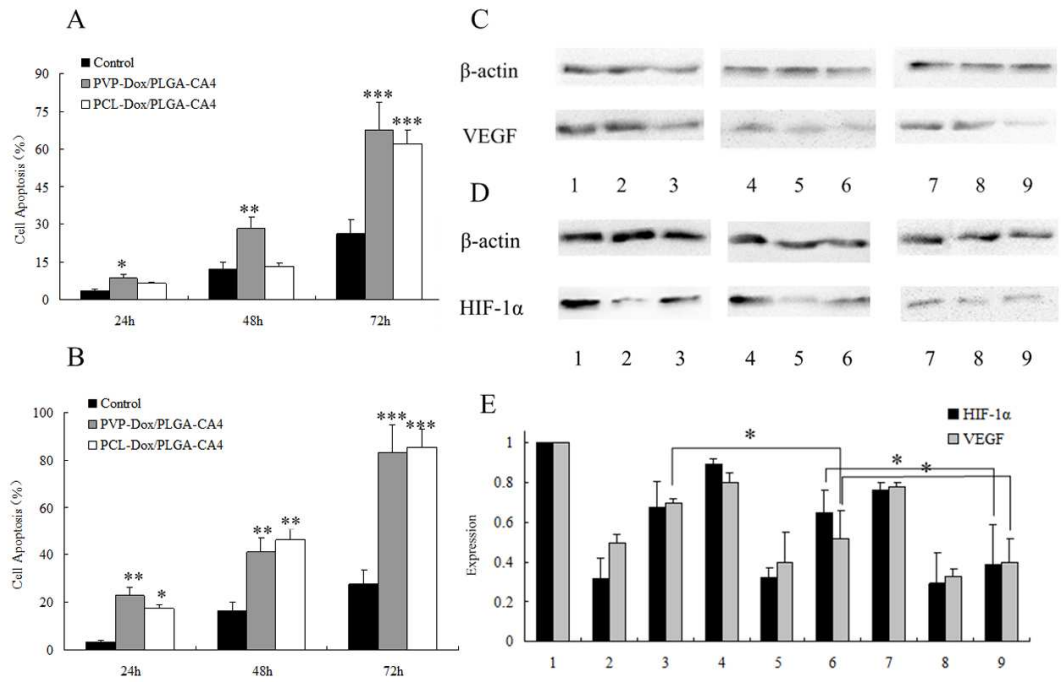

Fig.7 A-B) Cell apoptosis of nanoparticles after incubation with co-culture cells systems *in vitro* A: B16-F10 cell; B: EA.HY926 cell; C-D) HIF-1α and VEGF protein expressions of each sample in B16-F10 cells after different incubation time; E) Relative HIF-1α and VEGF protein expressions of each sample in B16-F10 cells after different incubation time; 1-3) 24h 1: Control; 2: PVP-DOX/PLGA-CA4; 3: PCL-DOX/PLGA-CA4; 4-6) 48h 4: Control; 5: PVP-DOX/PLGA-CA4; 6: PCL-DOX/PLGA-CA4； 7-9) 72h 7: Control; 8: PVP-DOX/PLGA-CA4; 9: PCL-DOX/PLGA-CA4; (Relative expression is normalized to β-actin; expression is shown relative to 24h control group, normalized to 1.) (mean ± SD; n = 3) * P <0.05, ** P<0.01, *** P<0.001.